

Ultrathin cobalt phosphate enfolded with biomass-derived multishelled carbon onion as a proficient electrocatalyst for the oxygen evolution reaction and its green sustainability assessments

Sundarraaj Sriram, Bakthavachalam Vishnu and Jayaraman Jayabharathi*

Department of Chemistry, Material Science Lab, Annamalai University, Annamalai Nagar, Tamil Nadu-608 002, India

1. Experimental section

1.1 Materials and methods

Cobalt (II) nitrate ($\text{Co}(\text{NO}_3)_2 \cdot 6\text{H}_2\text{O}$), Potassium hydroxide, ammonium phosphate ($\text{NH}_4\text{H}_2\text{PO}_4$) and isopropanol were purchased from SDFCL chemicals; and double distilled DI water. Waste frying oil used for the synthesis of CNOs was collected from local food shop providing catering. Nickel foam was purchased from Vritra technologies Delhi India. These chemicals were used as received without further purification. Deionized (DI) water, ethanol, and 3 M HCl were used as solvents and for washing. The Ni foam (thickness: 0.5 mm) was purchased from Vritra technologies Delhi India.

1.2 Synthesis of onion like carbon

The onion like carbon/carbon nano onions (OLC/CNOs) were synthesized by simple and catalyst-free process (Flame pyrolytic technique) using waste frying oil as the carbon source. About 30 ml waste oil was poured into the spirit lamp with cotton wick ($d = 0.5$ mm). One end of the cotton wick was immersed in the oil and another end was exposed to the ambient condition through a nozzle, cotton wick was ignited under ambient condition. The black soot was collected by using copper plate, placed just above the tip of the flame and the carbon powder was scrapped off (Figure 1: step 1). The cost-effective flame pyrolytic technique method is capable of producing CNOs at a rate of the order of grams per hour (Figure S1).

1.3 Synthesis of carbon nano onions wrapped cobalt phosphate

The CPCs were synthesized by having the weight ratio of P-Co-C as 400-500-50, 400-400-50 and 500-400-50 by varying the components in milligrams and it denoted as CPC 4-5, CPC 4-4, CPC 5-4. By the mechanochemical process the carbon and cobalt was grained for 10 minutes and the ammonium phosphate was also added into it. Further it was grinded for 30 mins. The grinding reaction mixture was filtered with distilled H_2O and ethanol, then dried under the sunlight to form CPCs (Figure 1: step: 2). And also, for electro-active comparison

CoP (400-400), P-Co-Graphene (400-400-50) and P-Co-Graphite (400-400-50) catalyst were synthesised and it was named as CoP, Graphene 4-4 and Graphite 4-4.

1.4 Physical characterization

X-ray diffraction (XRD) of CPCs were recorded with Thermo XRD equinox 1000. Fourier transform infrared (FTIR) spectra of CPCs were recorded on Shimadzu IR Tracer-100. The morphology, elemental mapping and EDX of CPC 4-4 was determined by using ZEISS Sigma 300 field emission scanning electron microscope (FESEM). JEM-2100 Plus was used to record transmission electron microscope (TEM) image of the Carbon onion (C) and CPC 4-4 and selected area electron diffraction (SAED) pattern was taken from JEOL, JEM-2100 Plus. The elemental composition of CPC 4-4 was analyzed by XPS (X-ray photoelectron spectroscopy) with K-ALPHA SURFACE ANALYSIS spectrometer.

1.5 Electrocatalytic characterization

The catalytic performances of the electrodes for water oxidation were studied using three-electrode configuration connected to Biologic Electrochemical Workstation SP-200 potentiostat at room temperature. The CPCs and IrO₂ on glassy carbon electrode and on nickel foam (NF) were used as the working electrodes. The Ag/AgCl (sat. KCl) electrode and Pt wire were used as the reference and counter electrodes. The working NF electrode was washed with 1 M HCl to remove oxide layer on the nickel surface, then washed with water and acetone and dried. The slurry was prepared by mixing 4.0 mg of catalyst in 1.0 ml solvent mixture of Nafion (5 wt %) and water in v/v ratio of 1/9 for 20 min. in an ultrasonicator. Commercially available catalyst (IrO₂) and bare NF was used. About 1.0 mg/ml of commercial IrO₂ suspension was prepared by following the similar methodology for comparison and bare NF was used directly. The slurry was drop casting on a precleaned NF electrode and the electrode was allowed to dry at 70°C before measurement (catalyst loading 0.5 mg cm⁻²). The freshly synthesized catalyst and commercial IrO₂ catalyst have been used directly as working electrode without further

treatment. All measurements were carried out in 1.0 M KOH (aq). The OER activities of CPCs have been analyzed by OER polarization curves (LSV), electrochemical impedance spectroscopy (EIS) and chronopotentiometry. The OER activity of the catalyst have been made by linear sweep voltammetry (LSV) on NF electrode (scan rate: 10 mV s⁻¹). The impedance of each catalyst was measured by electrochemical impedance spectroscopy (EIS) over a frequency range of 100 kHz to 10 mHz with sinusoidal perturbation amplitude of 0.5 V. Here, the turnover frequency (TOF) rate of evolved molecular O₂ per surface active site per second can be calculated. The overpotential used for the calculation of TOF was set at potential of 1.6 V vs RHE [3]. The TOF can be calculated using the equation $TOF = [J \times A / 4 \times F \times n]$ where, J- Current density, A- Area, F- Faraday Constant, n- the number of moles in catalyst. $RF = ECSA/GSA$ (RF- roughness factor, ECSA- electrochemical surface area and GSA- Geometric surface area)

Figure S1. Mechanism of CNOs formation by flame pyrolysis of waste fry oil

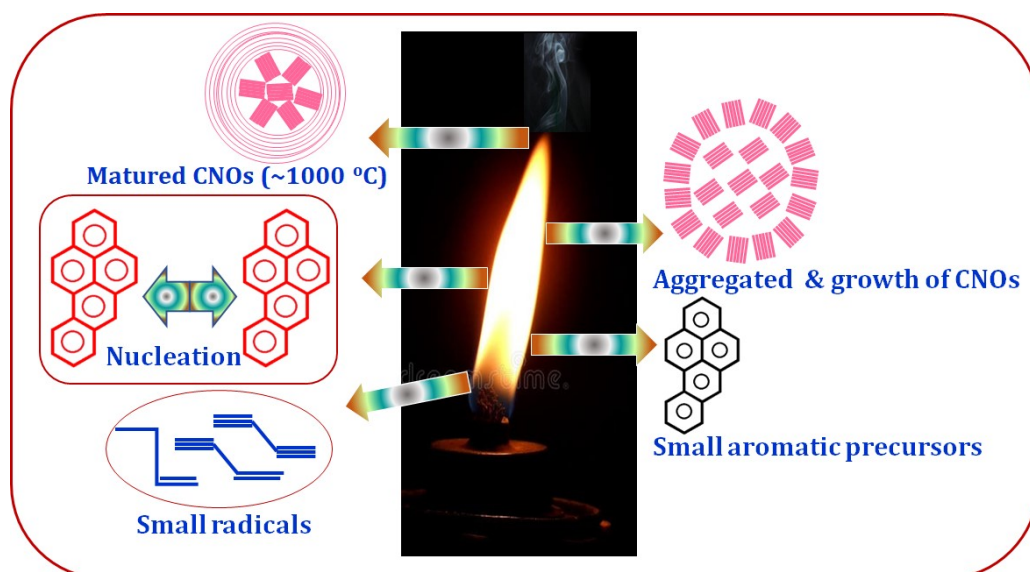


Figure S2. Raman spectroscopy of C, CPC 4-5, CPC 4-4 and CPC 5-4.

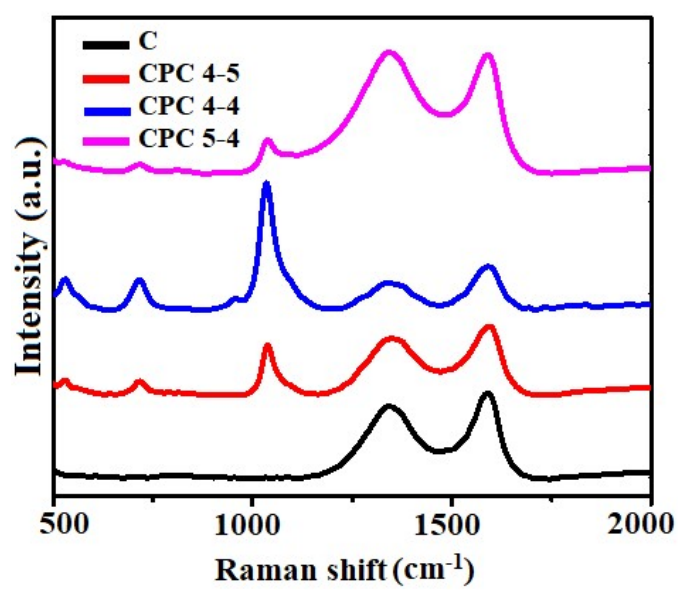


Figure S3. FE-SEM of CPC 4-4: (a, b) EDX spectrum and (c-g) FE-SEM elemental mapping

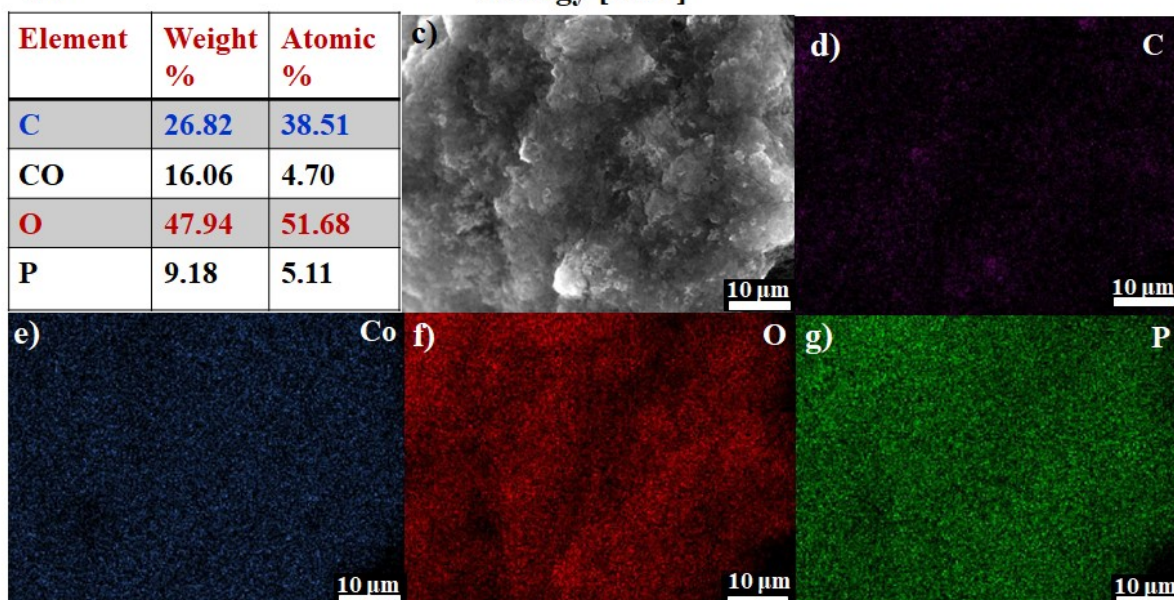
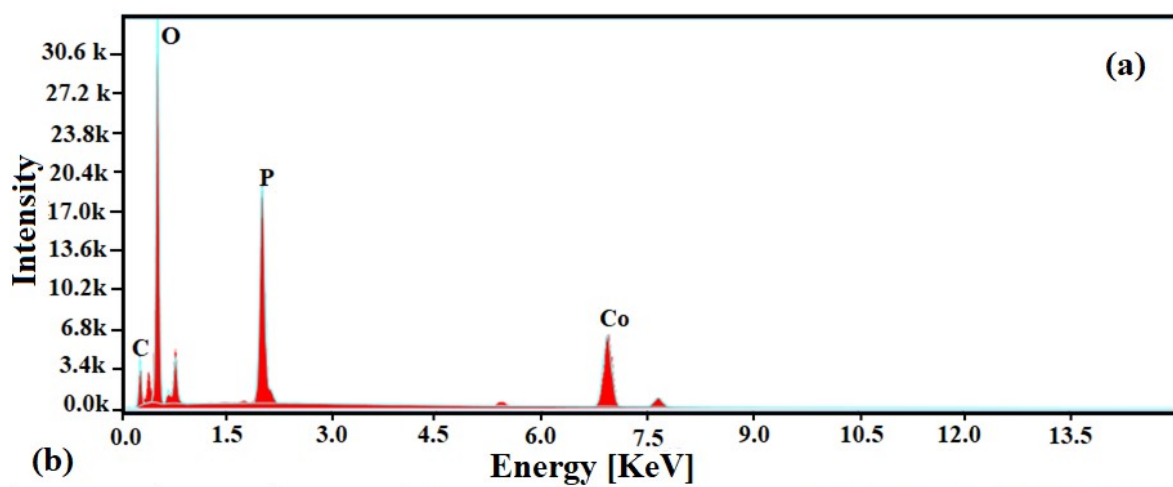


Figure S4. Survey spectra of CPC 4-4

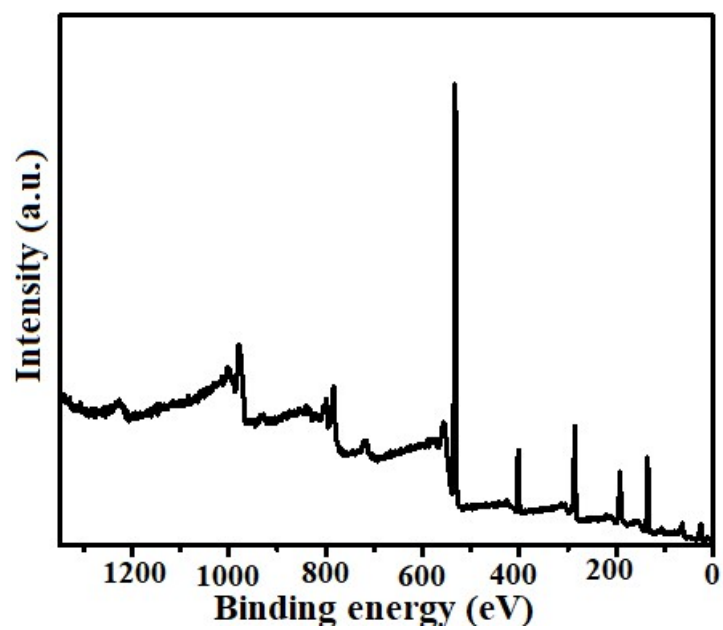


Figure S5. LSV curve of CPC 4-4 in different loading amount in GC

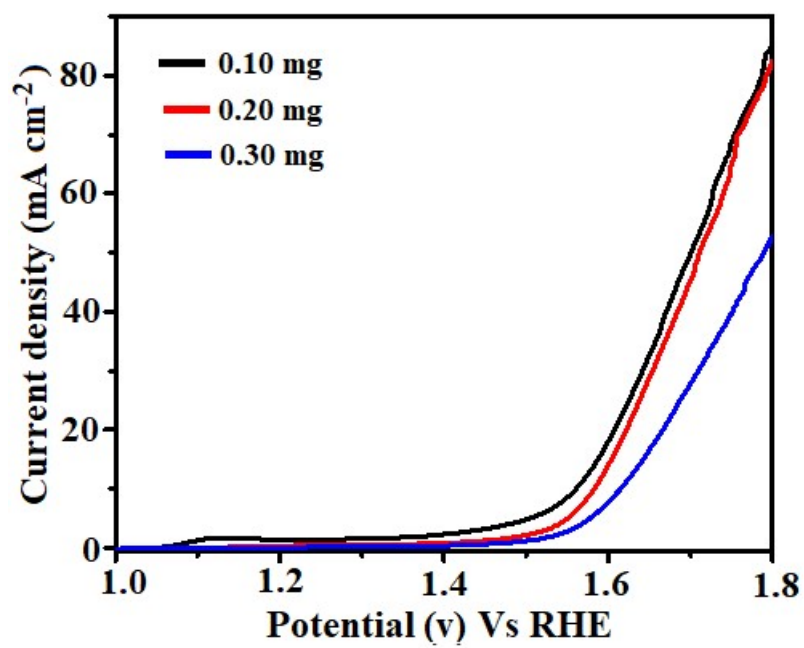


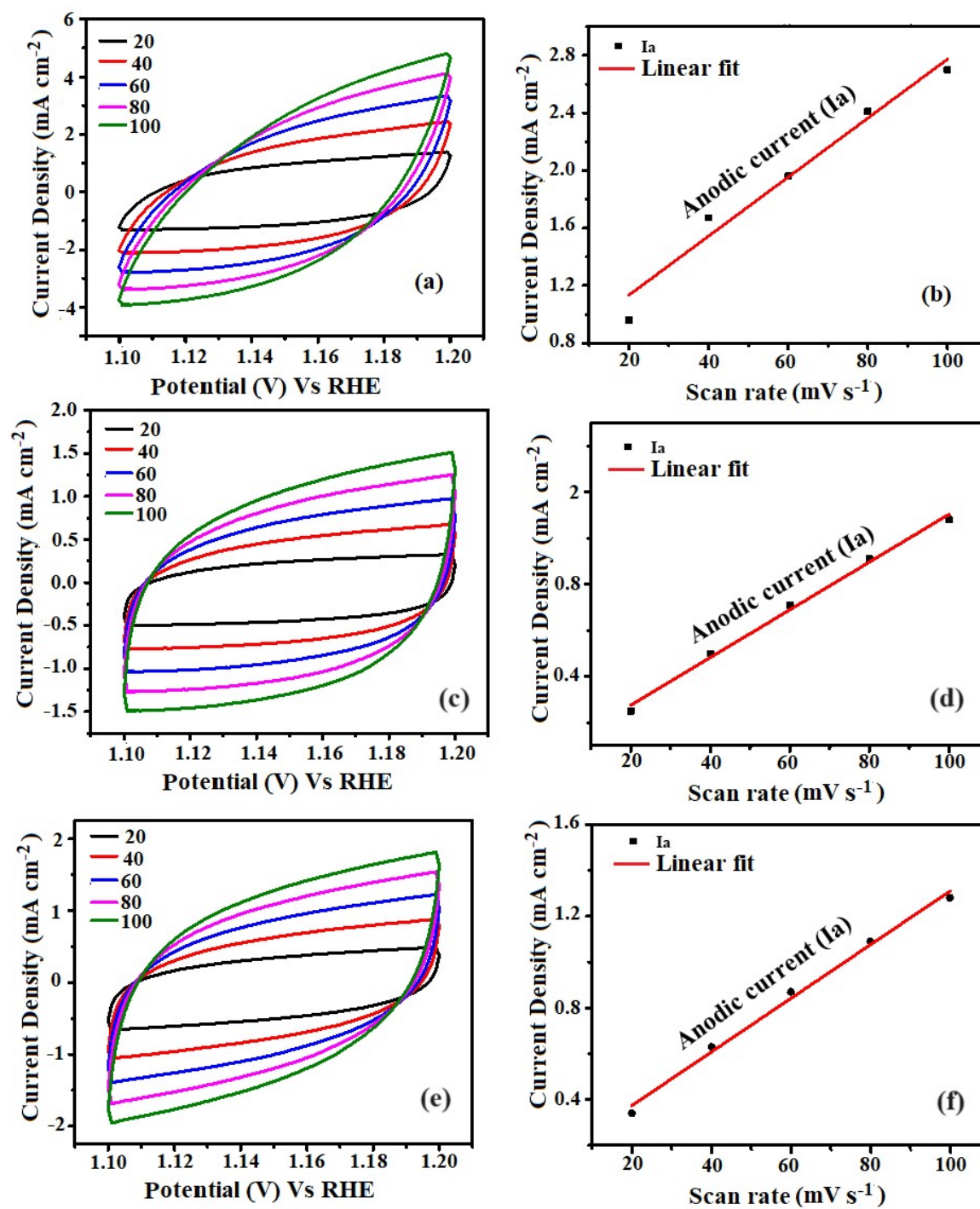
Figure S6. ECSA of CPC 4-5, CPC 5-4 and IrO₂.

Figure S7. Post-XRD analysis of the CPC 4-4

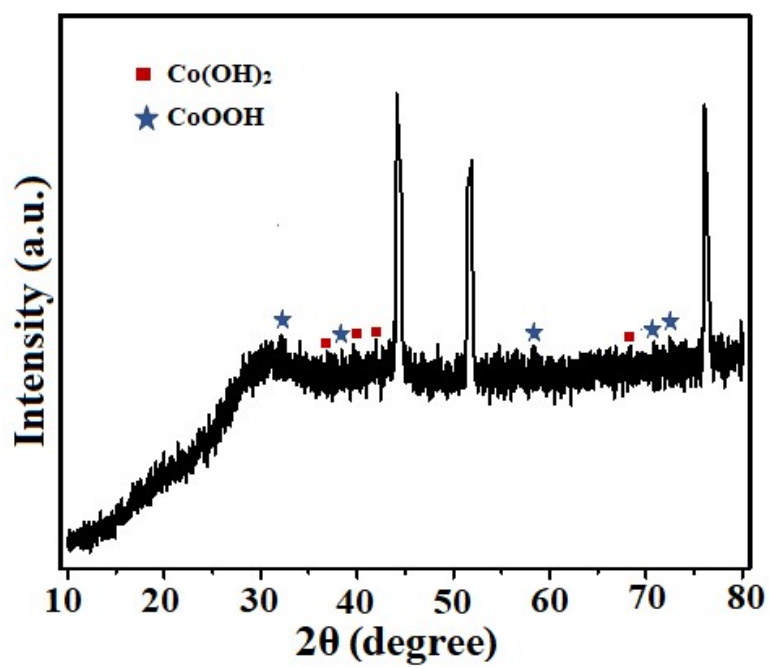


Figure S8. Post-FE-SEM analysis of the CPC 4-4

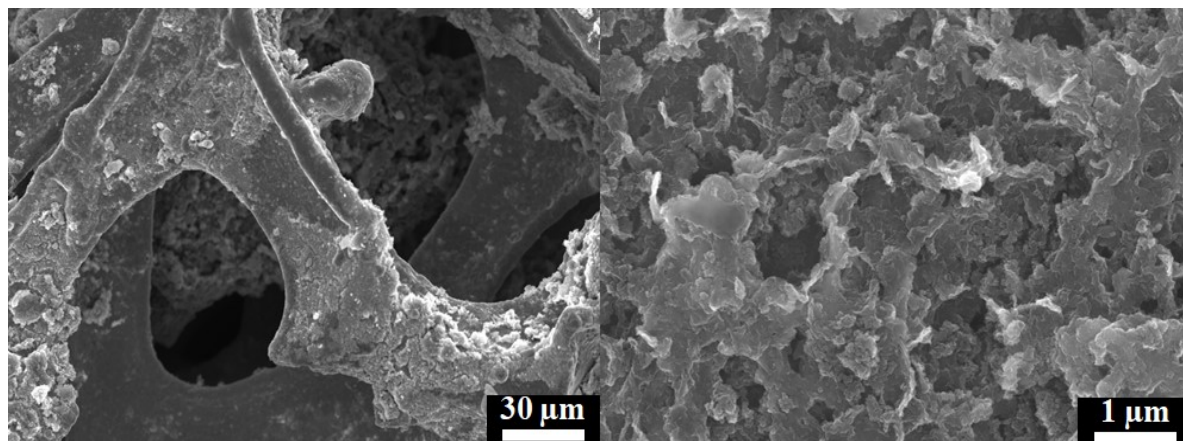


Figure S9. Post-FE-SEM of CPC 4-4: (a) EDX spectrum and (b-g) FE-SEM elemental mapping.

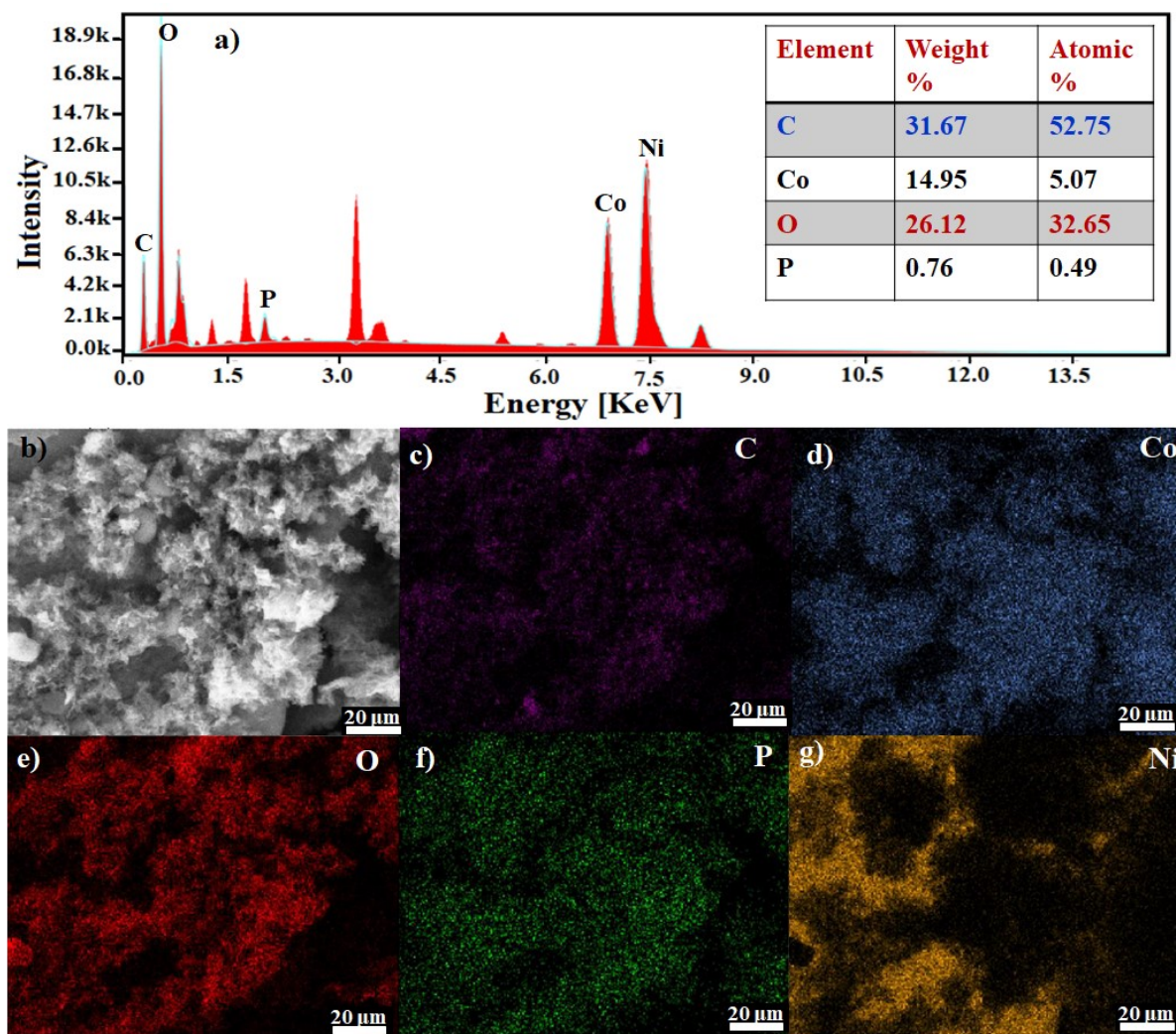


Figure S10. Post-XPS spectra of the CPC 4-4

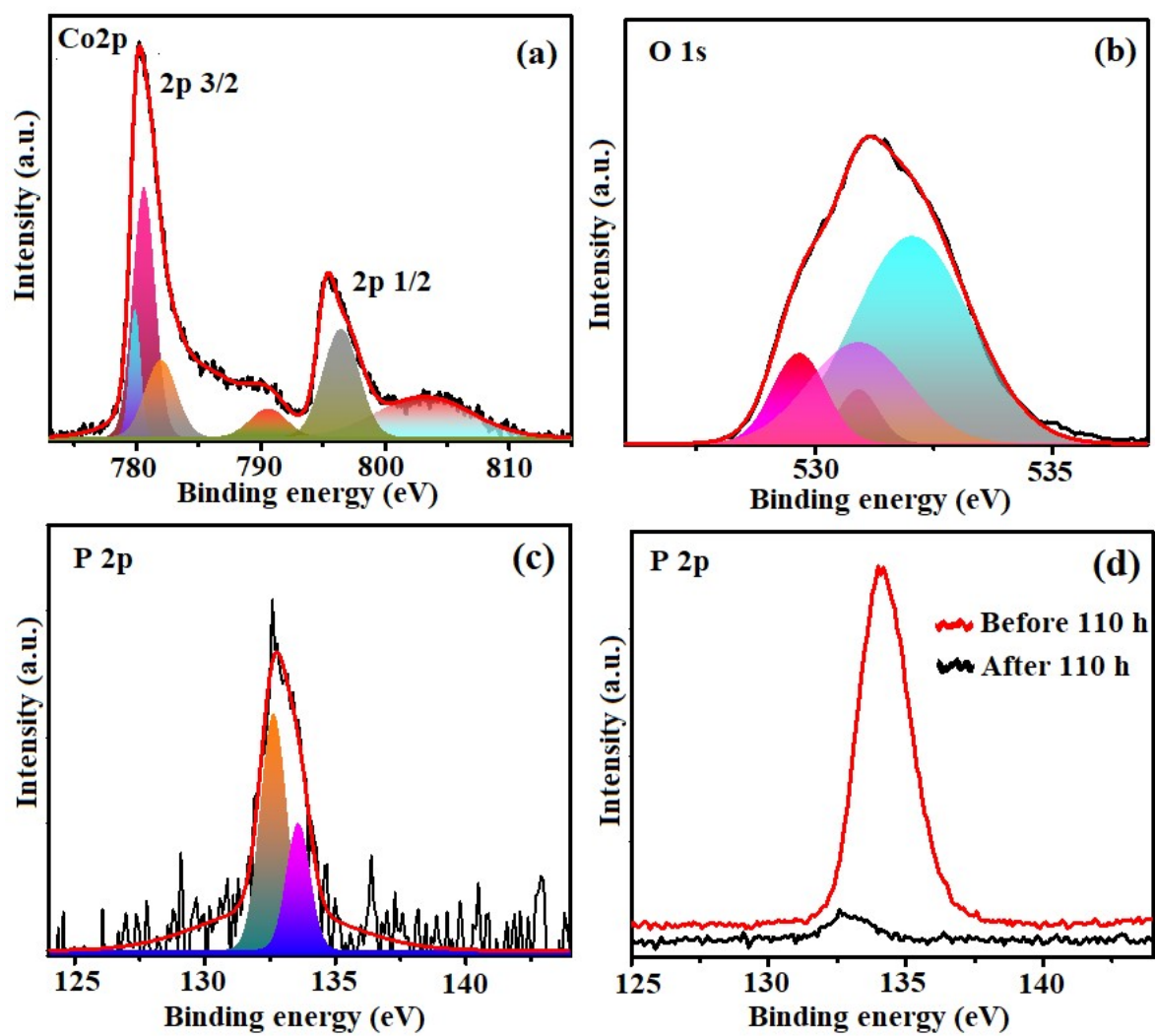
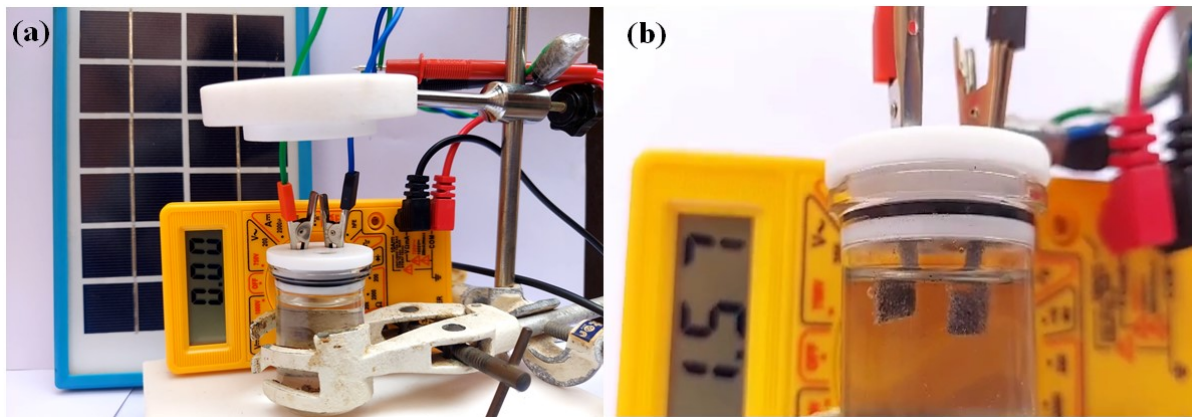


Figure S11: Solar cell water electrolyzer for hydrogen production (CPC4-4/NF// Pt/C/NF) at 1.57V.



S1.1. Calculation of hydrogen generation

Based on the displaced amount of water due to the hydrogen bubbles the amount of hydrogen generated was calculated using the below relationships.

$$\text{Amount of hydrogen generated in 1 h} = \text{amount of water displaced in litres} \quad (1)$$

$$\left. \begin{array}{l} \text{Amount of hydrogen generated} \\ \text{in moles for 1 h} \end{array} \right\} = \frac{\text{Amount of water displaced (liters)}}{22.4 \text{ liters}} \quad (2)$$

We also calculated the hydrogen generation rate from the electrical charge passed through the electrode using the equation given below.

$$\begin{array}{l} \text{Current obtained} \\ \text{During water electrolysis} \end{array} \times \begin{array}{l} \text{Time duration for} \\ \text{each potential} \end{array} = \text{Coulomb} \quad (3)$$

$$\frac{\text{Coulomb} \times F}{96485C} = \text{No. of moles of e- for H}_2 \text{ generation} \quad (4)$$

$$\left. \frac{\text{No. of moles of electron for H}_2 \text{ generation} \times 1 \text{ mole of H}_2 \text{ gas}}{2 \text{ mole of electron}} \right\} = \text{Moles of Hydrogen generated} \quad (5)$$

SI.2. Environmental impact assessment

Equation S1

$$\text{Mass Intensity} = \frac{\text{Mass of all reactants used excluding water}}{\text{Mass of product}} \text{kg/kg product}$$

Equation S2

$$\text{Water Intensity (Wp)} = \frac{\text{Mass of all water used}}{\text{Mass of product}} \text{kg/kg product}$$

Equation S3

$$\text{Reaction Mass Efficiency (RME)} = \frac{\text{Mass of product}}{\text{Mass of all reactants}} \times 100\%$$

Equation S4

$$\text{Energy Intensity} = \frac{\text{Amount of non renewable energy used}}{\text{Mass of product}} \text{kW.h/kg}$$

Equation S5

$$E \text{ factor} = \frac{[\text{kg}(\text{raw material}) - \text{kg}(\text{desired product})]}{[\text{kg}(\text{total product including water})]}$$

Table S1. Comparison of OER performance of CPC 4-4 with recently reported transition metal phosphate-based catalysts.

Catalyst	Support	Electrolyte	Over potential (mV)	Ref
CPC 4-4	GC	1 M KOH	301	This work
	NF	1 M KOH	271	
CoP	GC	1 M KOH	400	[1]
Fe-P nanotube	Carbon cloth	1 M KOH	461	[2]
Co-P-derived films	Cu foil	1 M KOH	413	[3]
(Ni,Co) ₃ Si ₂ O ₅ (OH) ₄ : PO ₄	GC	1 M KOH	394	[4]
Co@NPC	CC	1 M NaOH	360	[5]
Ni/Ni ₂ P/Mo ₂ C@C	GC	1 M KOH	368	[6]
Ni ₁ Co ₁ P	GC	1 M KOH	343	[7]
Fe ₁ Co ₂ -P/C	RDE	1 M KOH	362	[8]
Ir-Co MOF@600	GC	1 M KOH	317	[9]
Ni ₂ P/rGO	GC	1 M KOH	320	[10]
N-CoO@CoP@NF	NF	1 M KOH	332	[11]
CoP hollow polyhedron	GC	1 M KOH	400	[12]
NiCoP/C nanoboxes	GC	1 M KOH	330	[13]
Ni ₂ P-CoP	GC	1 M KOH	320	[14]
CoP/rGO hybrids	GC	1 M KOH	340	[15]
Ni ₂ P nanosheets	GC	1 M KOH	347	[16]
carbon fiber paper@FeP	GC	1 M KOH	350	[17]
MnCoP nanoparticles	GC	1 M KOH	330	[18]
NiCoP microspheres	GC	1 M KOH	340	[19]
FeCo/Co ₂ P	GC	1 M KOH	330	[20]

Table S2. ECSA and roughness factor for electrocatalysts

Catalysts	ECSA (m²/g)	Roughness factor (rf)
CPC 4-5	50	708.21
CPC 4-4	90.5	1274.78
CPC 5-4	25	354.10
IrO ₂	29.2	413.59

Table S3. Comparison of overall water splitting performance of CPC 4-4/NF//Pt/C/NF with recently reported electrocatalysts.

Material	Electrolyte (KOH)	Over potential @10 mA cm⁻²	Substrate	Ref.
CPC 4-4	1.0 M	1.57 V	NF	This work
Co(OH) ₂ @NCNTs@NF	1.0 M	1.72 V	NF	[3]
CP/CTs/Co-S	1.0 M	1.74 V	Carbon paper	[21]
Ni ₃ S ₂ /NF	1.0 M	1.76 V	NF	[22]
Co-P film	1.0 M	1.74 V	Copper foil	[23]
Co-Fe Composite film	1.0 M	1.68 V	Carbon paper	[24]
NiCo alloy	1.0 M	1.68 V	NF	[25]
CoP/PNC	1.0 M	1.68 V	PNC	[26]
LiCoBPO	1.0 M	1.84 V	NF	[27]
NiCoFeB nanochains	1.0 M	1.81 V	CFP	[28]
NiFe ₂ O ₄ /VACNT	1.0 M	1.72 V	VACNT	[29]
Ni-P film	1.0 M	1.67 V	Copper foil	[30]
PO-Ni/Ni-N-CNFs	1.0 M	1.69 V	CFP	[31]
Cop/MoP@NC/CC	1.0 M	1.71 V	CC	[32]
NiFe/NiCo ₂ O ₄ /NF	1.0 M	1.67 V	NF	[33]
Cop/MoP@NC/CC	1.0 M	1.71 V	CC	[34]
NiCo ₂ O ₄ @NiO@Ni	1.0 M	1.60 V	NF	[35]

Table S4. Comparison of solar to hydrogen efficiency of CPC 4-4 with recently reported electrocatalyst

Electrocatalysts	STH Efficiency (mmol h⁻¹ cm⁻²)	Reference
CPC 4-4	4.91	This Work
Fe-PANI	4.57	[36]
Co@SPANI-800	3.91	[37]
Co ₄ Ni ₁ @PANI	4.03	[38]
RCFC-10	4.51	[39]
Co@PANI-600	4.01	[40]

Table S5. Mass-based sustainability metrics evaluation for the synthetic process of the CPC4-4

Material	Mass intensity (MI) (kg/kg)	Solvent intensity (SI) (kg/kg)	Reaction mass efficiency (RME) %	Energy consumption (kW·h/kg)	E-factor
CPC 4-4	4.2	96	23.5	0	1.3

Reference

- [1] M. Liu, J. Li, *ACS Appl. Mater. Interfaces.*, 2016, **8**, 2158-2165.
- [2] Y. Yan, B. Y. Xia, X. Ge, Z. Liu, A. Fisher, X. Wang, *Chem.-Eur. J.*, 2015, **21**, 18062-18067.
- [3] N. Jiang, B. You, M. Sheng, Y. Sun, *Angew. Chem.*, 2015, **127**, 6349- 6352.
- [4] C. Qiu, L. Ai, J. Jiang., *ACS Sustainable Chem. Eng.*, 2018, **6**, 4492-4498.
- [5] K. Nath. D. Bhunia. Pradhan. and K. Biradha. *Nanoscale Adv.*, 2019, **1**, 2293-2302.
- [6] X. Li, X. Wang, J. Zhou, L. Han, C. Sun, Q. Wang, and Z. Su, *J. Mater. Chem. A.*, 2018, **6**, 5789-5796.
- [7] C. Shuai, Z. Mo, X. Niu, P. Zhao, Q. Dong, Y. Chen, N. Liu, and R. Guo, *J. Electrochem. Soc.*, 2020, **167**, 026512.
- [8] W. Hong, M. Kitta, and Q. Xu, *Small Methods*, 2018, **2**, 1800214-1800219.
- [9] C. H. Liao, K. Fan, S. S. Bao, H. Fan, X. Z. Wang, Z. Hu, M. Kurmoo, and L. M. Zheng, *Chem comm.*, 2019, **55**, 13920-13923.
- [10] L. Yan, H. Jiang, Y. Xing, Y. Wang, D. Liu, X. Gu, P. Dai, L. Li, and X. Zhao, *J. Mater. Chem. A.*, 2018, **6**, 1682-1691.
- [11] M. Lu, L. Li, D. Chen, J. Li, N. I. Klyui, and W. Han, *Electrochim. Acta.*, 2020, **330**, 135210 - 135239.
- [12] M. Liu and J. Li, *ACS Appl. Mater. Interfaces.*, 2016, **8**, 2158-2165.
- [13] P. He, X. Y. Yu, and X. W. Lou, *Angew. Chem., Int. Ed.*, 2017, **56**, 3897-3900.
- [14] X. Liang, B. Zheng, L. Chen, J. Zhang, Z. Zhuang, and B. Chen, *ACS Appl. Mater. Interfaces.*, 2017, **9**, 23222-23229.
- [15] L. Jiao, Y. X. Zhou, and H. L. Jiang, *Chem. Sci.*, 2016, **7**, 1690-1695.
- [16] Z. Li, X. Dou, Y. Zhao, and C. Wu, *Inorg. Chem. Front.*, 2016, **3**, 1021-1027.

- [17] D. Xiong, X. Wang, W. Li, and L. Liu, *ChemComm.*, 2016 **52**, 8711-8714.
- [18] D. Li, H. Baydoun, C. N. Verani and S. L. Brock *J. Am. Chem. Soc.*, 2016. **138**, 4006-4009.
- [19] C. Wang, J. Jiang, T. Ding, G. Chen, W. Xu, and Q. Yang, *Adv. Mater. Interfaces*, 2016, **3**, 1500454-1500458.
- [20] X. Han, S. J. Zhou, Y. Z. Tan, X. Wu, F. Gao, Z. J. Liao, R. B. Huang, Y. Q. Feng, X. Lu, S. Y. Xie, and L. S. Zheng, *Angew. Chem., Int. Ed. Engl.*, 2008, **47**, 5340-5343.
- [21] P. Guo, J. Wu, X. B. Li, J. Luo, W. M. Lau, H. Liu, X. L. Sun, L. M. Liu, *Nano Energy*, 2018, **47**, 96-104.
- [22] X. B. Zhang, J. Wang, H. X. Zhong, Z. L. Wang, F. L. Meng, *ACS Nano.*, 2016, **10**, 2342-2348.
- [23] L. L. Feng, G. Yu, Y. Wu, G. D. Li, H. Li, Y. Sun, T. Asefa, W. Chen, X. Zou, *J. Am. Chem. Soc.*, 2015, **137**, 14023-14026.
- [24] N. Jiang, B. You, M. Sheng, Y. Sun, *Angew. Chem.*, 2015, **127**, 6349-6352.
- [25] W. Liu, K. Du, L. Liu, J. Zhang, Z. Zhu, Y. Shao, M. Li, *Nano Energy*, 2017, **38**, 576-584.
- [26] B. Zhang, X. Zhang, Y. Wei, L. Xia, C. Pi, H. Song, Y. Zheng, B. Gao, J. Fu, P. K. Chu, *J. Alloys Compd.*, 2019, **797**, 1216-1223.
- [27] Z. Peng, Y. Yu, D. Jiang, Y. Wu, B. Y. Xia, Z. Dong, *Carbon*, 2019, **144**, 464-471.
- [28] P. W. Menezes, A. Indra, I. Zaharieva, C. Walter, S. Loos, S. Hoffmann, R. Schlögl, H. Dau, M. Driess, *Energy Environ. Sci.*, 2019, **12**, 988-999.
- [29] Y. Li, B. Huang, Y. Sun, M. Luo, Y. Yang, Y. Qin, L. Wang, C. Li, F. Lv, W. Zhang, S. Guo, *Small*, 2019, **15**, 1804212.
- [30] R. Li, X. Li, D. Yu, L. Li, G. Yang, K. Zhang, S. Ramakrishna, L. Xie, S. Peng, *Carbon*, 2019, **148**, 496-503.

- [31] Y. Xu, Y. Yan, T. He, K. Zhan, J. Yang, B. Zhao, K. Qi, B. Y. Xia, *Carbon*, 2019, **145**, 201-208.
- [32] N. Jiang, B. You, M. Sheng, Y. Sun, *ChemCatChem.*, 2016, **8**, 106-112.
- [33] Z. Y. Wu, W. B. Ji, B. C. Hu, H. W. Liang, X. X. Xu, Z. L. Yu, B. Y. Li, S. H. Yu, *Nano Energy*, 2018, **51**, 286-293.
- [34] Y. J. Tang, H. J. Zhu, L. Z. Dong, A. M. Zhang, S. L. Li, J. Liu, Y. Q. Lan, *Appl. Catal. B.*, 2019, **245**, 528-535.
- [35] L. Wang, C. Gu, X. Ge, J. Zhang, H. Zhu, and J. Tu, 2017. *Part Part Syst Charact.*, **34**, 1700228-1700237.
- [36] B. Vishnu, S. Sriram, and J. Jayabharathi, *New J. Chem.*, 2023, **47**, 5977-5990.
- [37] M. Vijayarangan, S. Mathi, A. Gayathri, J. Jayabarathi, and V. Thanikachalam, *ChemistrySelect*, 2022, **7**, 202203206-202203219.
- [38] V. Ashok, S. Mathi, M. Sangamithirai, and J. Jayabharathi, *Energy Fuels*, 2022, **36**, 14349-14360.
- [39] B. Vishnu, S. Mathi, S. Sriram, B. Karthikeyan, and J. Jayabharathi, *Energy Fuels*, 2022, **36**, 1654-1664.
- [40] S. Sriram, S. Mathi, B. Vishnu, B. Karthikeyan, B. and J. Jayabharathi, *ChemistrySelect*, 2022, **7**, 202104516.